 e-ISSN: 2686-2573
DOI: 10.21512/emacsjournal.v8i2.16476

2006 Yogyakarta Synthetic Time History Response Spectrum versus SNI 1726:2019: Building Response

Abdul Rozaq[1*], Jafar[2], Elvis Saputra[3]

[1-3]Department of Civil Engineering, Faculty of Engineering Design Innovation,
Islamic University of Indonesia
Sleman-Yogyakarta, Indonesia 55584
abdulrozaq2k4@gmail.com; jafar@uii.ac.id; elvis.saputra@uii.ac.id

[*]Correspondence: abdulrozaq2k4@gmail.com

Abstract – *This study investigates how a response spectrum derived from a synthetic acceleration time history representing the 2006 Yogyakarta earthquake compares with the SNI 1726:2019 design spectrum and influences the seismic response of a five-story reinforced concrete building. A 5%-damped event-based spectrum was developed through linear-acceleration analysis of single-degree-of-freedom systems and applied alongside the SNI spectrum to a three-dimensional ETABS model for Site Class SD. The developed spectrum reached a peak pseudo spectral acceleration of 1.011 g at 0.34 s, exceeding the SNI plateau of 0.78 g (0.155–0.777 s) by 29.62%. At the building's fundamental period of 1.086 s in X, the developed and SNI spectra gave 0.58 g and 0.56 g, a difference of 3.51%. At 1.385 s in Y, they gave 0.32 g and 0.44 g, a difference of 31.58%. The corresponding differences in unscaled base shear, elastic roof displacement, maximum inter-story drift, and P-Delta stability coefficients were small in X (2.28–3.05%) but greater in Y (27.35–31.34%), where SNI generally produced higher demands. Force scaling brought all cases to 2961.020 kN, although story-level force distributions remained different. All drift and stability checks met the adopted limits. These findings indicate that period-dependent spectral differences are reflected in structural responses but remain specific to the synthetic input and building examined. Further studies using additional ground motions and different building configurations are recommended.*

Keywords: *2006 Yogyakarta earthquake; Synthetic time history; Response spectrum; Fundamental period; SNI 1726:2019*

I. INTRODUCTION

Indonesia is in a seismically active zone due to the interaction of the major tectonic plates and buildings and infrastructure are therefore exposed to a high level of earthquake hazard. The 27 May 2006 Yogyakarta earthquake was a major event which did a great deal of damage and clearly demonstrated the fragility of RC structures to strong ground shaking. Pawirodikromo (2014) looked at the engineering characteristics of the ground motions associated with that earthquake and their impact on the inelastic response of RC structures. Hanniel et al., (2021) went on to look at the event via strong ground motion simulation using the empirical Green's function method. That work forms the basis for an understanding of the characteristics of the Yogyakarta earthquake and the relationship between earthquake ground motion and structural response.

Response spectrum analysis is the method of choice in earthquake resistant structural design for the estimation of seismic demand via the use of a design response spectrum which is a function of the structure's natural vibration period. In Indonesia, SNI 1726:2019 provides design response spectra based on seismic hazard parameters and site classifications as part of the standard requirements for earthquake resistant building design (Badan Standardisasi Nasional, 2019). The spectral characteristics of a code based design response spectrum will be different to those of a response spectrum derived from a single earthquake ground motion. Gülkan et al., (2023) looked at the response spectrum shapes associated with earthquakes in Turkey and compared these with the design spectra. Guzel & Guzel, (2023) looked at the European and Turkish code-based design spectra and Guzel & Güzel, (2024) looked at the inclusion of site effects in design response spectra. These studies all underline the importance of looking at the differences between the spectral representations when assessing seismic demand. It is important to note however that a response spectrum derived from

Copyright © 2026

a single earthquake event should not be taken as a hazard consistent site specific design spectrum as they are fundamentally different in their purpose and in the basis on which they are developed.

Earlier work has looked at the development of response spectra from recorded or simulated earthquake ground motions. Kristiyanto et al., (2022) developed elastic response spectra for the Mamuju earthquake and looked at the implications for building design in Indonesia. Rifaldy & Sukamdo, (2025) developed response spectra from the Palu 2018 earthquake time-history data by numerically integrating SDoF systems. There have also been a number of international studies looking at the relationship between ground motion characteristics and spectral demand. Papazafeiropoulos & Plevris, (2023) processed the strong motion records from the February 2023 Kahramanmaras earthquakes to produce elastic and constant ductility response spectra and incremental dynamic analysis curves.(Zengin et al., 2025) developed inelastic response spectra from both recorded and simulated ground motions in order to assess the spatial distribution of earthquake damage potential. Ulza et al., (2025) also looked at various computational approaches to response spectrum analysis. All of these studies demonstrate the value of numerical spectrum development and the use of time-history data in the assessment of seismic demand. The generation of a spectrum from a single event is of course a very different proposition to the construction of a representative design spectrum from a number of records or the evaluation of a regional seismic hazard.

Beyond the issue of spectral development, there have been studies looking at the impact of alternative spectral representations on structural design and building response. Khatiwada et al., (2023) compared site-specific response spectra with code-based response spectra as part of a dynamic modal analysis of building structures. The study illustrates the significance of the spectrum selection in the assessment of structures, although their site-specific spectral approach is different to that of an event-based spectrum derived from a single synthetic time history. In Indonesia, Sakul et al., (2025) have compared the local spectral response obtained via PSHA, the Indonesian design spectra and SNI 1726:2019 in the structural evaluation of an RC building. Prajapati et al., (2026) have developed response spectra from 19 ground motion records from the 2015 Gorkha earthquake sequence, compared these spectra with the Nepalese and Indian design spectra and then assessed the seismic response of an RC building model using ETABS. These studies show that the comparison of earthquake-derived and code-based spectra can be extended to the level of building assessment. They also show that the use of a 3d building model in itself is not the novelty of the present study.

For the 2006 Yogyakarta earthquake Pawirodikromo, (2014) reported on the digitisation and spectral matching of ground motion estimates that had previously been published and then went on to examine the inelastic response of an RC frame. That work is of course very pertinent to the ground motion literature that forms the basis of the present study. The aims of the present work are however very different. We are not claiming to produce a new Yogyakarta earthquake record or to develop a new ground motion reconstruction technique. Rather we are taking the synthetic time history input that has been used in the current analysis and using it to generate an event based response spectrum. We then compare that event based response spectrum with the SNI 1726:2019 design response spectrum and assess the impact of the two on a 3D multi-degree-of-freedom (MDoF) RC building model. That is an extension of the work from the planar RC frame to a comparison of the force, deformation and stability demands in both principal directions of a spatial building system.

The actual significance of using a response spectrum generated from a synthetic time history of the 2006 Yogyakarta earthquake (in conjunction with the SNI 1726:2019 design response spectrum) to a 3D RC building model is not really addressed in any of the literature we've looked at. The issue isn't simply that the two spectra have different acceleration values. It's about what those differences actually mean in terms of the seismic demand on the structure. Differences in the spectra at the building's natural vibration periods will have an impact on base shear, the distribution of seismic story forces, story shear, lateral displacement, inter-story drift and P-Delta. With a 3d model you can look at these responses in both principal directions and take into account the differences in stiffness and dynamic behaviour in the two directions. That gives you a much more complete picture of the relationship between spectral characteristics and building response than simply a comparison of the spectral curves.

The study is intended to (1) generate a response spectrum from a synthetic time history that represents the 2006 Yogyakarta earthquake; (2) compare this response spectrum to the design response spectrum as specified in SNI 1726:2019; and (3) assess the impact of the differences between the two on the seismic response of a 3d RC building model. The evaluation of the structural response will be in terms of base shear, seismic story forces, story shear, lateral displacement, inter-story drift and P-Delta. The study is framed around three research questions: (1) What are the differences in the spectral characteristics between the response

spectrum derived from the synthetic Yogyakarta time history and the SNI 1726:2019 design response spectrum? (2) What effect do these differences have on the force, deformation and stability responses of the 3d building model? (3) How do the resulting structural demands compare prior to and after scaling of the response spectrum analysis results? The purpose of the study is to determine the implications of using an event-based response spectrum in place of the code-based design response spectrum for the assessment of seismic demand on the building model in question. The conclusions of the study are not intended to be generalised to all earthquake scenarios and the comparison of the two response spectra is not intended to be a complete assessment of the adequacy of SNI 1726:2019.

II. METHODS

2.1 Research and Analytical Workflow

This computational study consisted of two stages. First an event-based response spectrum was created from the acceleration time history that represents the 2006 Yogyakarta earthquake. A single-degree-of-freedom (SDoF) system was examined over a range of natural vibration periods to obtain displacement (SD) pseudo spectral velocity (PSV) and pseudo spectral acceleration (PSA). Second the developed response spectrum was compared with the design response spectrum specified in SNI 1726:2019 and both response spectra were applied to a multi-degree-of-freedom (MDoF) reinforced concrete building model. The SDoF calculations were carried out in Microsoft Excel while the structural modelling, modal analysis and response spectrum analysis were performed in ETABS version 22. The structural responses were evaluated in the X and Y directions.

The workflow included consistency checks for the SDoF calculations generation of the SNI design spectrum, from its seismic parameters and modal validation of the three-dimensional building model. The cumulative modal participating mass was required to exceed 90% in each direction before the response spectrum analysis was conducted.

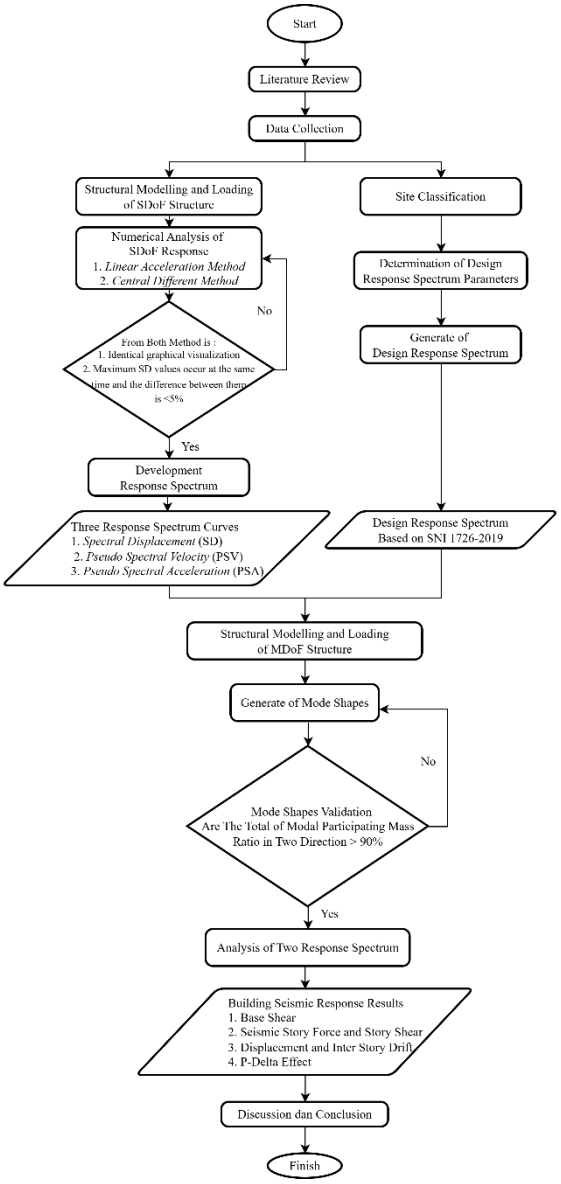


Figure 1. Computational workflow for developing the 5%-damped response spectrum from the synthetic 2006 Yogyakarta earthquake time history and comparing building responses with SNI 1726:2019.

Once the modal validation criteria had been met, response spectrum analyses were performed on the 3D MDoF building model by applying both the event-based response spectrum and the SNI 1726:2019 design response spectrum in turn to the X and Y directions. The structural responses from the analyses were extracted from ETABS 22 and the base shear, seismic story forces, story shear, lateral displacement, inter-story drift and the P-Delta stability coefficient were all assessed. The results from the two response spectra were then compared to determine the differences in seismic demand and structural response in each of the principal directions. The force scaling, displacement amplification and stability assessment were all

carried out in accordance with the relevant provisions of SNI 1726:2019 as outlined in the following methodological sections. The numerical results were then interpreted in the context of the research objectives and previous work, which formed the basis for the discussion, conclusions and identification of the study's limitations.

2.2 Earthquake Time-History Input and Data Provenance

The earthquake data used in this study was a set of acceleration records that showed what happened during the 2006 Yogyakarta earthquake. This data was given by the research supervisor. Was credited to Pawirodikromo, (2014). The acceleration data was used as it was without any changes for making the response spectrum. No extra work was done to convert the seismogram into form or to match it with any other spectrum in this study.

The details of the acceleration time history, such as how the data was recorded how many points there were, how long the data lasted, the highest acceleration values, the peak ground acceleration (PGA) and how long the ground shook strongly are listed in Table 1. These details describe the data used in the analysis.

Table 1. Characteristic of synthetic time history Yogyakarta earthquake 2006 by Pawirodikromo, (2014)

Parameter	Value	unit
Duration	40	s
Time step	0.01	s
Number of samples	4000	unit
Maximum acceleration	+305.5613	cm/s^2
	-330.8897	cm/s^2
PGA	0.3373	g
Effective duration, D_{5-95}	12.38	s

The documents that are available do not explain the way the data was converted into digital form how the movement of the ground was oriented, how the baseline was corrected or the reference spectrum the method used the range of periods and the allowed error that was used for any previous matching of spectra. Because of that these steps in processing cannot be checked on their own. Are not said to have been done in this study. Also it was not possible to find out how the acceleration data provided relates to the ground-motion record mentioned by Pawirodikromo, (2014) based on the documents available.

Only one acceleration time history was available, without a separately identified orthogonal horizontal component. The developed response spectrum was therefore applied independently in the X and Y directions of the building model, rather than representing simultaneous bidirectional ground-motion excitation. Koz et al., (2025) examined the influence of bidirectional earthquake motions on structural response, highlighting an aspect that could not be evaluated using the available data. Accordingly, the developed spectrum represents the response to the supplied synthetic Yogyakarta earthquake time history and should not be interpreted as a hazard-consistent, site-specific design spectrum.

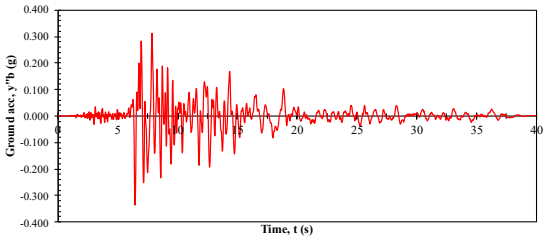


Figure 2. Synthetic 2006 Yogyakarta earthquake acceleration time history attributed to Pawirodikromo, (2014), with a 40 s duration, 0.01 s time step, and peak ground acceleration of 0.3373 g.

2.3 Development of the Event-Based Response Spectrum

The response spectrum was calculated by analysing linear elastic SDoF systems subjected to the supplied ground acceleration. For a system with mass (m), damping coefficient (c), stiffness (k), and relative displacement y(t), a unit mass (m=1) was used for the SDoF system to simplify the numerical work. For a linear elastic system under base excitation the mass can be eliminated from the equation of motion by dividing through by m. The displacement response is then a function of the natural vibration period, the damping ratio and the ground acceleration input rather than the absolute value of the mass. The stiffness and damping coefficient were therefore defined in accordance with the specified natural period and damping ratio.

$$\mathrm{m}\ddot{\mathrm{y}} + c\dot{\mathrm{y}} + \mathrm{k}\mathrm{y} = -\mathrm{m}\ddot{\mathrm{y}}_t \quad (1)$$

$$\omega = \frac{2\pi}{\mathrm{T}} = \sqrt{\frac{k}{m}} \quad (2)$$

$$\mathrm{c} = 2\xi\mathrm{m}\omega \quad (3)$$

A damping ratio of 5% is used, as the SDOF structure is assumed to be ordinary concrete with minor cracking (Pawirodikromo, 2017). The linear acceleration method and central difference method were used to compute the SDoF response. For the linear acceleration method, the equation used is as follows:

$$\ddot{\mathrm{y}}_{(\mathrm{i}+1)} = \frac{6}{\Delta \mathrm{t}^2}\left(\mathrm{y}_{(\mathrm{i}+1)} - \mathrm{y}_\mathrm{i} - \Delta \mathrm{t}\dot{\mathrm{y}}_\mathrm{i} - \frac{\Delta \mathrm{t}^2}{3}\ddot{\mathrm{y}}_\mathrm{i}\right) \quad (4)$$

$$\dot{\mathrm{y}}_{(\mathrm{i}+1)} = \frac{3}{\Delta \mathrm{t}}(\mathrm{y}_{(\mathrm{i}+1)} - \mathrm{y}_\mathrm{i}) - 2\dot{\mathrm{y}}_\mathrm{i} - \frac{\Delta \mathrm{t}}{2}\ddot{\mathrm{y}}_\mathrm{i}) \quad (5)$$

$$\mathrm{y}_{(\mathrm{i}+1)} = \frac{-\mathrm{m}\ddot{\mathrm{y}}_{b(i+1)} - \mathrm{a}\mathrm{y}_i - \mathrm{b}\dot{\mathrm{y}}_i + c_1\ddot{\mathrm{y}}_\mathrm{i}}{\hat{k}} \quad (6)$$

$$\hat{k} = \frac{6m}{\Delta \mathrm{t}^2} + \frac{3c}{\Delta \mathrm{t}^2} + k \quad (7)$$

$$\mathrm{a} = \frac{6m}{\Delta \mathrm{t}^2} + \frac{3c}{\Delta \mathrm{t}} \quad (8)$$

$$b = \frac{6m}{\Delta t} + 2c \quad (9)$$

$$c_1 = 2m + c\frac{\Delta t}{2} \quad (10)$$

For the central difference method, the displacement recurrence as below:

$$y_{(i+1)} = \frac{-m\ddot{y}_{bi} - ay_i - by_{(i-1)}}{\hat{k}} \quad (11)$$

$$\hat{k} = \frac{m}{\Delta t^2} + \frac{c}{2\Delta t} \quad (12)$$

$$a = k - \frac{2m}{\Delta t^2} \quad (13)$$

$$b = \frac{m}{\Delta t^2} - \frac{c}{2\Delta t} \quad (14)$$

The stability of both methods is expressed by the following equation:

$$\frac{\Delta t}{T} \leq \frac{1}{\pi} \text{ for linear acceleration, and} \quad (15)$$

$$\frac{\Delta t}{T} \leq \frac{3}{\pi} \text{ for central difference} \quad (16)$$

We carried out response analysis by stepping through natural periods in 0.02 second increments beginning at 0.02-6 s. At the short period of 0.02 s the central difference method failed to meet the numerical stability criterion so we had to drop it, but for periods of 0.04 s and longer the central difference method did meet the stability requirement and we kept it for comparison with the linear acceleration method. Even though we looked at both methods in their ranges we chose the linear acceleration method to find the final maximum absolut displacement for every national period. We then used those SD values to compute the pseudo velocity or PSV and the pseudo spectral acceleration or PSA.

Validation was performed by comparing the displacement time history of the single-degree-of-freedom (SDoF) system subjected to the synthetic Yogyakarta 2006 earthquake acceleration record, calculated using the linear acceleration and central difference methods. Visual inspection of the overlaid displacement curves indicated a high degree of agreement between the two numerical solutions.

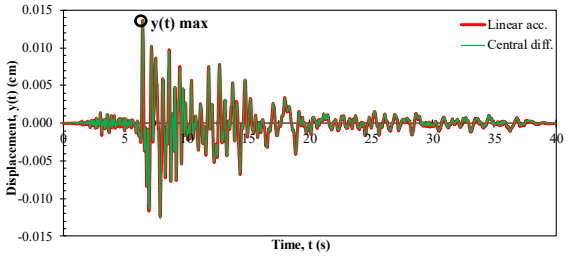


Figure 3. Comparison of relative SDoF displacement time histories calculated using the linear acceleration and central difference methods at T = 0.04 s and 5% damping.

Quantitative validation was conducted by calculating the relative difference between the maximum absolute displacements obtained from both methods. As neither method was designated as the reference solution, the average of the two maximum absolute displacement values was used as the denominator.

$$\Delta\% = \frac{(SD_1 - SD_2)}{\frac{(SD_1 + SD_2)}{2}} x100\% \leq 5\% \quad (17)$$

This criterion was used to assess the consistency of the calculated displacement responses and support the selection of the linear acceleration method for determining the final spectral displacement (SD) values. Suwito (2024) also demonstrated the use of computational tools for generating earthquake response spectra, highlighting the role of numerical procedures in spectral analysis. However, the comparison between the two numerical methods in the present study was intended to assess internal computational consistency rather than provide independent validation against an external reference solution.

Table 2. Spectral displacement validation sample

T (s)	SD_1 (cm)	SD_2 (cm)	Δ(%)
0.04	0.01366	0.01361	0.436
0.06	0.03046	0.03031	0.512
0.26	1.15730	1.18108	2.034
0.5	5.83193	5.84301	0.19
1	17.03281	17.05461	0.128
2	14.58097	14.58567	0.032
3	23.80726	23.81339	0.026
4	33.63295	33.63705	0.012
5	24.84758	24.85049	0.012
6	15.42780	15.42850	0.004

For PSV and PSA calculated were found using these formulas in every increments natural period 0.02 s:

$$PSV = SD x \omega \quad (18)$$

$$PSA = SD x \omega^2 \quad (19)$$

2.4 Response Spectrum Design by SNI 1726:2019

The earthquake design response spectrum based on code was created following SNI 1726:2019. It uses the site class and the earthquake parameters that were used in the study as Table 3 below:

Table 3. SNI 1726:2019 Seismic parameters

Parameter	Value	unit
Risk category	II	-
Ie	1	-
R	8	-
Ω_0	3	-
Cd	5,5	-
S_S	1.107	g
S_1	0.507	g
F_a	1.057	-
Fv	1.793	-
S_{MS}	1.17	g

S_{M1}	0.909	g
S_{DS}	0.78	g
S_{D1}	0.606	g
T_0	0.155	s
Ts	0.777	s
T_L	6	s
Design seismic category	D	-
ρ	1.3	-

2.5 Three-Dimensional Building Model

A five-storey reinforced concrete building special moment resisting frame (SMRF), with an inter-storey height of 4.2 m in Yogyakarta was modelled as a three-dimensional MDoF structure using ETABS version 22 is shown in Figure 5. The structural materials consisted of concrete with a compressive strength of f'c 27 MPa and reinforcing steel with a yield strength of fy 420 MPa. The main structural elements included floor slabs with a thickness of 120 mm, a roof slab of 100 mm, all columns with dimensions of 600×600 mm, and various beam dimensions as Table 4 below:

Table 4. Beam Dimensions

Code	B (mm)	H (mm)	L (mm)
BI1	400	500	6000
BI2	500	700	7500
BI3	300	400	3000
BI4	400	500	5000
BA1	300	400	6000
BA2	400	500	7500
BA3	250	300	3000
BA4	300	400	5000

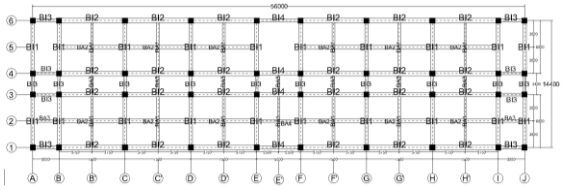


Figure 4. Plan view of the reinforced concrete beam layout used in the five-story building model; beam sizes and BI/BA codes are listed in Table 4.

Dead loads, superimposed dead loads, and live loads were assigned to the ETABS model in accordance with SNI 1727:2020 (Badan Standardisasi Nasional, 2020). The seismic mass source was defined using dead-load and superimposed dead-load patterns only, excluding live loads because the ratio of the storage live load to the effective seismic weight at each relevant floor level was below 5%, satisfying the exception specified in Section 7.7.2 of SNI 1726:2019, under which the additional 25% of floor live load in storage areas need not be included in the effective seismic weight. Nevertheless, live loads were retained as a separate load pattern in ETABS and included in the gravity-load calculations used to determine the total vertical load (Px) at and above each storey for the P-Delta stability evaluation. To account for the reduced flexural stiffness of reinforced concrete members, stiffness modifiers of 0.35, 0.70, and 0.25 were applied to the moments of inertia of beams, columns, and slabs, respectively. Rigid diaphragms were assigned at each floor level to represent in-plane floor rigidity, while fixed supports were specified at the column bases. Microsoft Excel was used for the SDoF numerical calculations and response spectrum development, whereas ETABS version 22 was used for three-dimensional structural modelling, modal analysis, and response spectrum analysis.

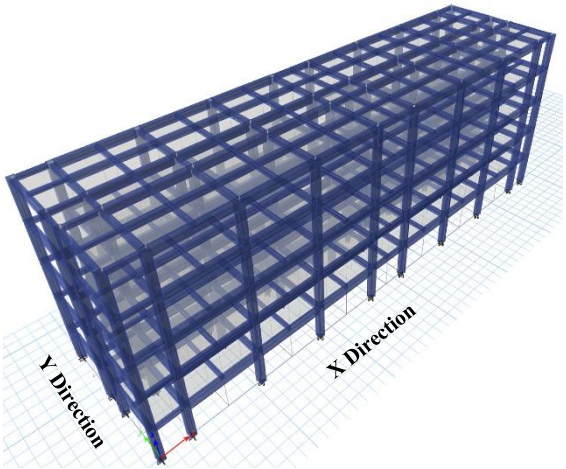
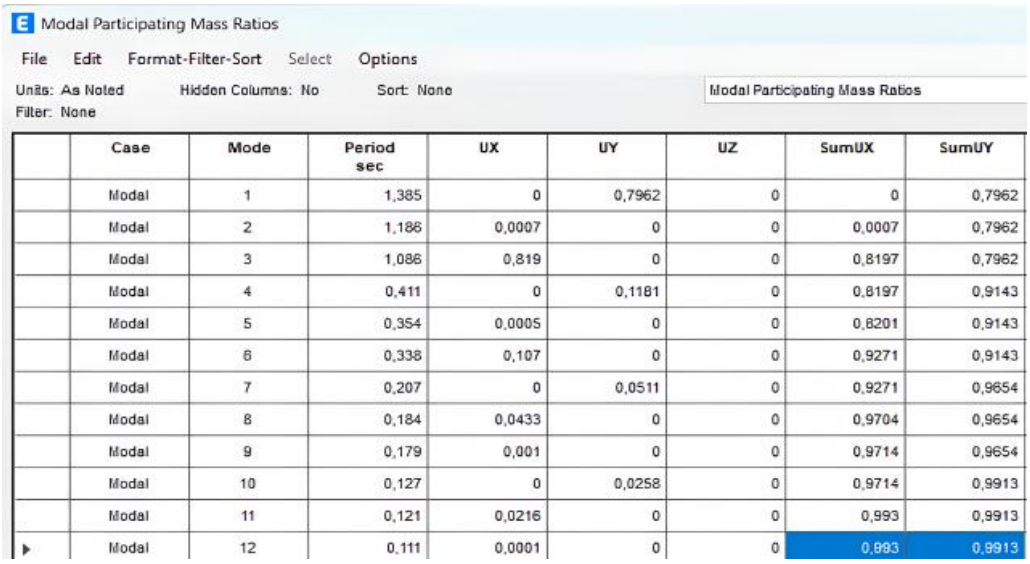


Figure 5. Three-dimensional ETABS model of the five-story reinforced concrete special moment-resisting frame, showing the X and Y principal directions and the 4.2 m story height.

2.6 Modal Analysis and Response Spectrum Analysis

Modal analysis was done in ETABS version 22 to find out the periods, mode shapes and modal participating mass ratios for the three-dimensional building. The number of modes was chosen in Figure 6 so that the total modal participating mass was than 90 percent in every main horizontal direction. This was in line, with the rule of SNI 1726:2019.



Modal Participating Mass Ratios

File Edit Format-Filter-Sort Select Options

Units: As Noted Hidden Columns: No Sort: None Modal Participating Mass Ratios

Filter: None

Case	Mode	Period sec	UX	UY	UZ	SumUX	SumUY
Modal	1	1,385	0	0,7962	0	0	0,7962
Modal	2	1,188	0,0007	0	0	0,0007	0,7962
Modal	3	1,086	0,819	0	0	0,8197	0,7962
Modal	4	0,411	0	0,1181	0	0,8197	0,9143
Modal	5	0,354	0,0005	0	0	0,8201	0,9143
Modal	6	0,338	0,107	0	0	0,9271	0,9143
Modal	7	0,207	0	0,0511	0	0,9271	0,9654
Modal	8	0,184	0,0433	0	0	0,9704	0,9654
Modal	9	0,179	0,001	0	0	0,9714	0,9654
Modal	10	0,127	0	0,0258	0	0,9714	0,9913
Modal	11	0,121	0,0216	0	0	0,993	0,9913
Modal	12	0,111	0,0001	0	0	0,993	0,9913

Figure 6. Modal natural periods and participating mass ratios of the five-story ETABS building model in the X and Y directions.

After finishing the modelling and modal analysis a response spectrum analysis was carried out using ETABS version 22. Two seismic input spectra were used. One was the event-based response spectrum, which came from the synthetic time history of the 2006 Yogyakarta earthquake. The other was the design response spectrum from SNI 1726:2019 applicable to Site Class SD. The modal analysis results were reviewed to make sure that the cumulative modal participating mass ratios were over 90%, in both horizontal directions. Each response spectrum was applied separately to the X-direction and Y-direction response spectrum load cases with a damping ratio set at 5%. The modal responses were combined using the method specified in the ETABS model. The final structural responses were assessed in both directions focusing on base shear seismic story forces, story shear, lateral displacement, inter-story drift and the P-Delta stability coefficient.

2.7 Equivalent Static Base Shear and Response Scaling

The equivalent static base shear was calculated in accordance with SNI 1726:2019 to establish the minimum base shear requirement for the response spectrum analysis. This was based on the effective seismic weight of the building (W) and the seismic response coefficient (Cs) which was derived from the relevant design spectral parameters and the structural period. The seismic base shear from ETABS was then compared to the equivalent static base shear to determine the required force scaling factor. The applicable upper and lower bounds of Cs were used in accordance with the SNI 1726:2019 requirements.

$$V_{static} = WxCs \quad (20)$$

$$C_S = \frac{S_{DS}}{\frac{R}{I_e}} \quad (21)$$

$$C_{Smax} = \frac{S_{D1}}{T\left(\frac{R}{I_e}\right)} \text{ for } T<T_L \quad (22)$$

$$C_{Smin} = 0.044 S_{DS} I_e \geq 0.01 \quad (23)$$

$$C_{Smin} = \frac{0.5 S_1}{\left(\frac{R}{I_e}\right)} \quad \text{for } S_1 \geq 0.6 \text{ g} \quad (24)$$

$$SF = \frac{Vstatic}{V_t} \quad \text{for } V_t < V_{static} \quad (25)$$

As per section 7.9.1.4.1 of SNI 1726:2019, additional displacement scaling is only required where the seismic base shear (V_t)< static base shear (V_{static}) and the seismic response coefficient (C_S) used to calculate V_{static} is that given by Equation (24) for locations where S_1 is greater than or equal to 0.6 g. Displacement scaling is therefore not always in conjunction with force scaling as the requirement for additional displacement scaling is dependent on the applicable seismic response coefficient. The elastic displacements from ETABS were then amplified by the deflection amplification factor (C_d/I_e) to obtain the inelastic displacements for the purpose of calculating inter-story drift and continue to calculating P-Delta stability coefficient.

$$\delta_x = \frac{C_d \delta_{xe.}}{I_e} \quad (26)$$

$$\Delta_x = \delta_{xi} - \delta_{x(i-1)} < \Delta_{limit} = \frac{0.02h}{\rho} \quad (27)$$

$$\Delta_{ratio} = \frac{\Delta x}{h} < \Delta_{ratio\ limit} = \frac{0.02}{\rho} \quad (28)$$

$$\theta = \frac{P_x I_{e\Delta}}{V_x h_{sx} C_d} < \theta_{max} = \frac{0.5}{\beta C_d} \leq 0.25 \quad (29)$$

III. RESULTS AND DISCUSSION

3.1 Response Spectrum Curves

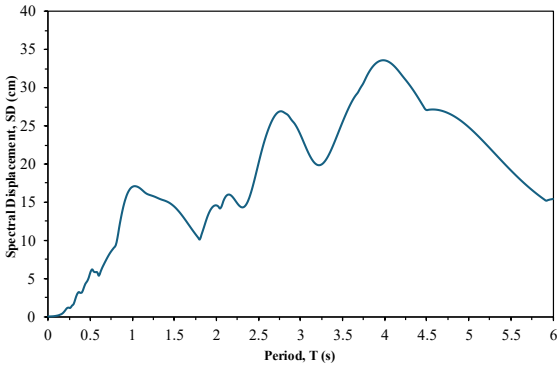


Figure 7. Spectral displacement (SD, cm) calculated from the synthetic Yogyakarta earthquake acceleration time history using the linear acceleration method at 5% damping.

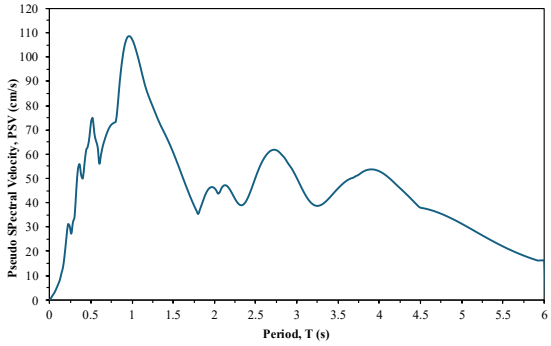


Figure 8. Pseudo spectral velocity (PSV, cm/s) calculated from the synthetic Yogyakarta earthquake acceleration time history at 5% damping.

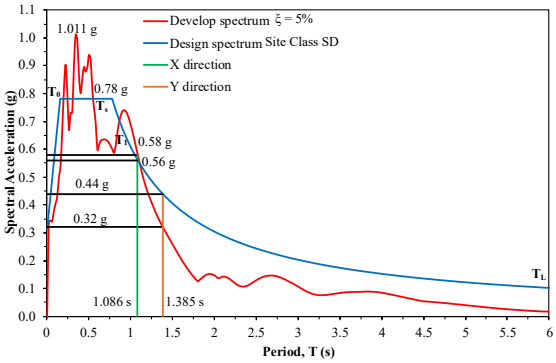


Figure 9. Comparison of 5%-damped pseudo spectral acceleration (PSA, g) for the developed Yogyakarta event-based spectrum and SNI 1726:2019 design spectrum (Site Class SD), with the X- and Y-direction fundamental periods marked.

The spectral displacement (SD) curve was developed from the maximum absolute SDoF displacement calculated using the linear acceleration method. Overall, SD increases with the natural vibration period, reaching approximately 33–34 cm at 3.8 s before decreasing to around 15 cm at 6.0 s. Several fluctuations appear along the curve, reflecting how the displacement response varies with the vibration period under the synthetic Yogyakarta earthquake input.

The pseudo spectral velocity (PSV) curve shows a different pattern, with a peak of approximately 110 cm/s at 0.9 s. After reaching this peak, PSV generally decreases, with some fluctuations at intermediate periods, to about 16 cm/s at 6.0 s. Unlike SD, PSV also depends on the natural circular frequency, which explains why its maximum occurs at a shorter vibration period.

A more noticeable difference appears when the developed pseudo spectral acceleration (PSA) spectrum is compared with the SNI 1726:2019 design spectrum for Site Class SD. At 5% damping, the developed spectrum reaches a peak of 1.011 g at 0.34 s, which is 29.62% higher than the SNI plateau of 0.78 g between 0.155 and 0.777 s. However, the developed spectrum does not remain higher throughout the period range, particularly at longer periods. Similar differences between earthquake-derived and design spectra have been discussed by Gülkan et al., (2023). (Budi et al., 2025) , meanwhile, reported recorded response spectra below the SNI design spectra for the earthquakes examined in their study. These findings suggest that the relationship between earthquake-derived and design spectra depends on the characteristics of the ground motion and the vibration period considered.

The comparison becomes particularly important at the building's fundamental periods. Based on the ETABS modal analysis, the fundamental periods are 1.086 s in the X direction and 1.385 s in the Y direction. At 1.086 s, the developed and SNI spectra give PSA values of 0.58 g and 0.56 g, respectively, with a difference of only 3.51%. In the Y direction, the difference is much greater, reaching 31.58%, as the developed spectrum gives 0.32 g compared with 0.44 g from the SNI spectrum. This suggests that the two spectra may produce relatively similar seismic demands in the X direction, while larger differences can be expected in the Y direction. However, the actual building response also depends on modal participation and the contribution of higher vibration modes, which are considered in the subsequent structural analyses.

3.2. Base Shear

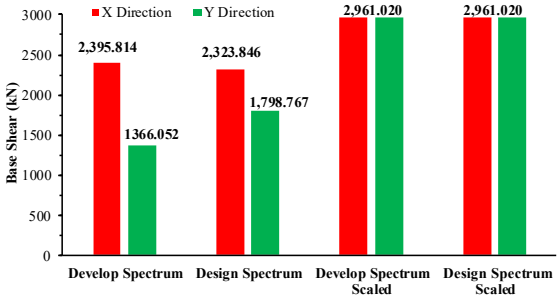


Figure 10. Unscaled and force-scaled seismic base shear (kN) in the X and Y directions for the developed and SNI 1726:2019 design response spectra.

Figure 10 compares the base shear obtained from the developed response spectrum and the SNI 1726:2019 design response spectrum. Before scaling, the developed spectrum produces 2395.814 kN in the X direction and 1366.052 kN in the Y direction, compared with 2323.846 kN and 1798.767 kN from the SNI spectrum. The differences are 3.05% in the X direction and 27.35% in the Y direction, calculated relative to the average of each pair. The relatively small difference in the X direction and the considerably larger difference in the Y direction are consistent with the spectral acceleration characteristics discussed in Section 3.1. In particular, the lower spectral acceleration of the developed spectrum in the Y direction is reflected in its lower base shear. Prajapati et al., (2026) also reported differences in base shear when earthquake-derived and code-based response spectra were used to analyse reinforced concrete buildings.

Since all unscaled base shear values were below the equivalent static requirement, scaling was applied in accordance with SNI 1726:2019. In the X direction, the scaling factor was 1.236 for the developed spectrum and 1.274 for the SNI design spectrum. In the Y direction, the factors were 2.168 for the developed spectrum and 1.646 for the SNI design spectrum. The larger factor required for the developed spectrum in the Y direction reflects its lower initial base shear. After scaling, all cases reached the required base shear of 2961.020 kN. This equality is a result of the scaling procedure and does not indicate identical structural responses.

3.3 Seismic Story Force and Story Shear

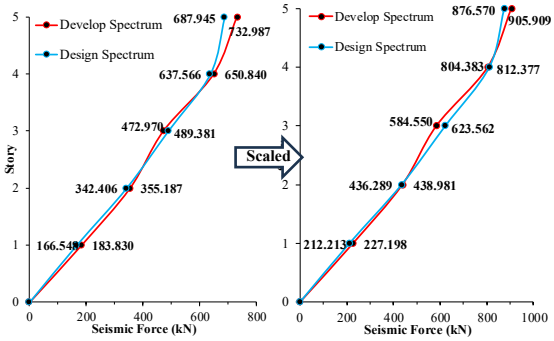


Figure 11. X-direction seismic story force distributions (kN) from the developed and SNI 1726:2019 design response spectra before and after force scaling.

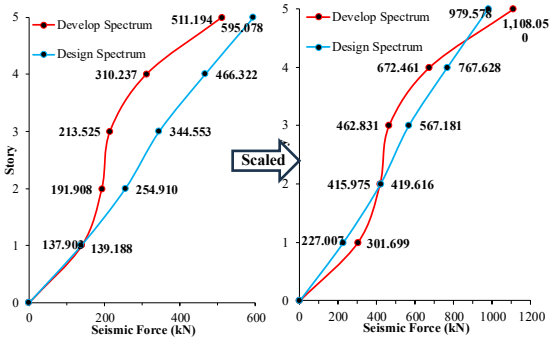


Figure 12. Y-direction seismic story force distributions (kN) from the developed and SNI 1726:2019 design response spectra before and after force scaling

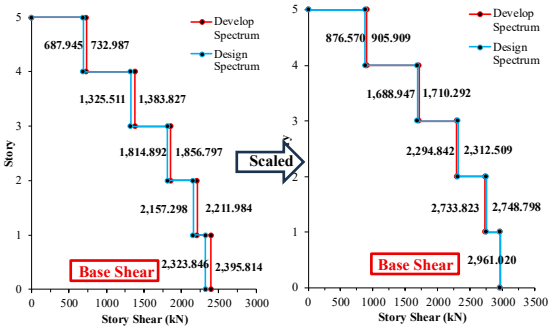


Figure 13. X-direction story shear distributions (kN) from the developed and SNI 1726:2019 design response spectra before and after force scaling

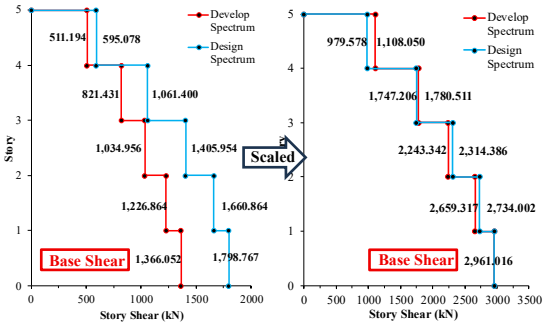


Figure 14. Y-direction story shear distributions (kN) from the developed and SNI 1726:2019 design response spectra before and after force scaling.

Figures 11 and 12 compare the seismic story forces obtained from the developed and SNI 1726:2019 design response spectra in the X and Y directions. Before scaling, both spectra generally produce higher forces toward the upper floors, although their values differ. At the fifth story in the X direction, the developed spectrum gives 732.987 kN, compared with 687.945 kN from the SNI spectrum, a difference of 6.34% relative to their average. In the Y direction, the opposite occurs: the SNI spectrum produces 595.078 kN, exceeding the developed spectrum value of 511.194 kN by 15.17%. These differences broadly follow the spectral acceleration characteristics at the building's fundamental periods, although the resulting story forces also depend on modal contributions.

After scaling, differences in story force distribution remain. In the X direction, the fifth-story forces become 905.909 kN and 876.570 kN for the developed and SNI spectra, respectively, with a difference of 3.29%. In the Y direction, the developed spectrum now produces a higher fifth-story force of 1108.050 kN, compared with 979.578 kN from the SNI spectrum, a difference of 12.31%. This reversal occurs because the developed spectrum requires a larger scaling factor in the Y direction (2.168) than the SNI spectrum (1.646). However, the SNI spectrum still produces higher forces at several intermediate floors, indicating that scaling does not eliminate differences in the vertical distribution of seismic forces.

Figures 13 and 14 show the corresponding story shear distributions, which increase toward the base as lateral forces accumulate from the upper floors. Although both spectra reach approximately 2961.020 kN at the base after scaling, their story shear values are not identical at every level. At the second story in the Y direction, for example, the difference decreases from 30.06% before scaling to 2.77% afterward. Khatiwada et al., (2023) also examined how different response spectra influence story shear demands in building structures. The present results similarly indicate that spectrum selection affects the distribution of seismic forces, even when the same minimum base shear is imposed. These differences reflect the combined influence of spectral characteristics, modal responses, and the scaling factors applied to each analysis case.

3.4 Displacement

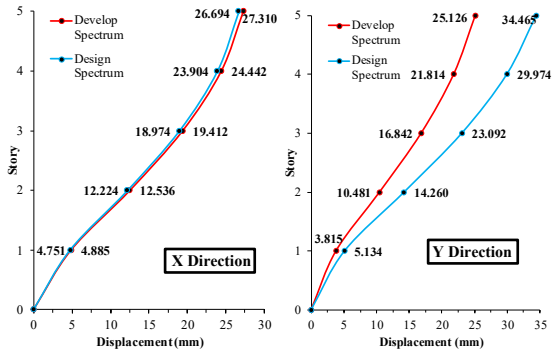


Figure 15. Unscaled elastic floor displacement profiles (mm) in the X and Y directions from the developed and SNI 1726:2019 design response spectra, before Cd/Ie amplification.

Figure 15 presents the elastic floor displacements obtained from the developed response spectrum and the SNI 1726:2019 design response spectrum using unscaled ETABS response spectrum load cases, without force scaling or (Cd/Ie) amplification. Both spectra produce increasing lateral displacements toward the roof, with the maximum values occurring at the fifth story. In the X direction, the developed spectrum gives 27.310 mm, slightly higher than the SNI value of 26.694 mm, with a difference of only 2.28% relative to their average. A larger difference occurs in the Y direction, where the SNI spectrum produces 34.465 mm, compared with 25.126 mm from the developed spectrum, corresponding to a difference of 31.34%.

The directional differences are consistent with the spectral acceleration characteristics discussed in Section 3.1, particularly the higher SNI spectral acceleration at the fundamental period in the Y direction. However, the resulting displacements also depend on the combined modal responses. Khatiwada et al., (2023) likewise reported variations in building displacement responses when different response spectra were applied, although their study used site-specific spectra rather than a spectrum derived from a single synthetic earthquake record. The present results therefore describe the elastic displacement response of the analysed building under the two spectral inputs. The amplified displacements used for inter-story drift and P-Delta evaluations are discussed separately in Sections 3.5 and 3.6.

3.5 Inter-Story Drift

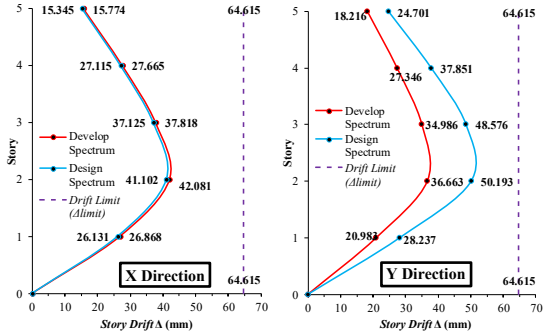


Figure 16. Design inter-story drift distributions (mm) in the X and Y directions from the developed and SNI 1726:2019 design response spectra, calculated using Cd/Ie-amplified displacements; dashed lines indicate the adopted 64.615 mm drift limit.

Table 5. Inter-story drift ratio

Story	Drift ratio				Limit
	X		Y		
	Develop	Design	Develop	Design	
5	0.0038	0.0037	0.0043	0.0059	0.0154
4	0.0066	0.0065	0.0065	0.0090	0.0154
3	0.0090	0.0088	0.0083	0.0116	0.0154
2	0.0100	0.0098	0.0087	0.0120	0.0154
1	0.0064	0.0062	0.0050	0.0067	0.0154

Figure 16 shows the inter-story drift distributions obtained from the developed and SNI 1726:2019 design response spectra, while the drift ratios are presented in Table 5. The drifts were calculated from the inelastic displacement estimates obtained by applying the (Cd/Ie) amplification factor to the elastic displacements discussed in Section 3.4. Both spectra show a similar pattern, with the highest drift occurring at the second story rather than at the roof. In the X direction, the developed spectrum gives a maximum drift of 42.081 mm, slightly above the SNI value of 41.102 mm, with a difference of 2.35% relative to their average. A greater difference appears in the Y direction, where the SNI spectrum produces 50.193 mm compared with 36.663 mm from the developed spectrum, corresponding to a difference of 31.16%. This pattern agrees with the spectral acceleration differences discussed earlier, particularly in the Y direction. The concentration of maximum drift at the second story may also be influenced by the distribution of story stiffness and modal deformation.

The drift ratios in Table 5 follow the same pattern, with maximum values occurring at the second story. In the X direction, the developed and SNI spectra give ratios of 0.0100 and 0.0098, respectively, reflecting the same 2.35% difference. In the Y direction, the corresponding ratios are 0.0087 and 0.0120, with a larger difference of 31.16%. All values remain below the adopted allowable ratio of 0.0154. Overall, both inter-story drift and drift ratio show relatively small differences between the spectra in the X direction, while the SNI spectrum produces considerably higher deformation demands in the Y direction. Nevertheless, both spectra satisfy the adopted drift criterion.

3.6 P-Delta Effect

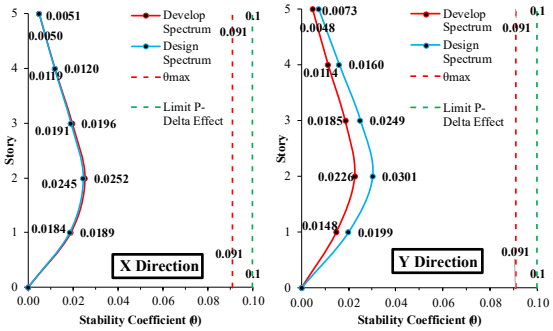


Figure 17. P-Delta stability coefficients (dimensionless) in the X and Y directions for the developed and SNI 1726:2019 design response spectra, calculated with force-scaled story shears and Cd/Ie-amplified design drifts; dashed lines show θmax = 0.091 and θ = 0.10.

Figure 17 presents the P-Delta stability coefficients (θ) obtained from the developed and SNI 1726:2019 design response spectra. Both spectra show a similar pattern, with the highest coefficients occurring at the second story. In the X direction, the developed spectrum gives a maximum coefficient of 0.0252, slightly higher than the SNI value of 0.0245, with a difference of 2.82% relative to their average. A larger difference appears in the Y direction, where the SNI spectrum produces 0.0301 compared with 0.0226 from the developed spectrum, corresponding to a difference of 28.46%. These differences are consistent with the inter-story drift results discussed in Section 3.5, particularly in the Y direction. However, the stability coefficient is also influenced by the gravity loads and story shears at each level.

For the stability check, SNI 1726:2019 specifies a threshold of θ = 0.10 below which P-Delta effects need not be considered. The maximum stability coefficient (θmax) determined for the building is 0.091, as established in the methodology. Since this value is lower than 0.10, it governs the stability assessment. All calculated coefficients remain below both limits, with the highest value of 0.0301 occurring under the SNI spectrum in the Y direction. Therefore, additional consideration of P-Delta effects is not required for the analysed building. Although all stability coefficients satisfy the adopted SNI 1726:2019 limits, this finding is limited to the linear response spectrum analysis. Türkay, (2026) reported higher structural demands from nonlinear time-history analysis than from linear response spectrum analysis, highlighting the need for further evaluation when assessing nonlinear seismic performance.

IV. CONCLUSION

The response spectrum developed from the synthetic 2006 Yogyakarta earthquake time history shows notable differences from the SNI 1726:2019 design response spectrum for Site Class SD. The developed spectrum reaches a peak pseudo spectral acceleration (PSA) of 1.011 g at 0.34 s, exceeding the SNI plateau of 0.78 g between 0.155 and 0.777 s by 29.62%. However, the differences vary with vibration period. At the building's fundamental period of 1.086 s in the X direction, the developed and SNI spectra give PSA values of 0.58 g and 0.56 g, respectively, with a difference of 3.51%. In the Y direction, at 1.385 s, the corresponding values are 0.32 g and 0.44 g, giving a larger difference of 31.58%. These findings indicate that the relative seismic demand between the two spectra depends on the vibration period considered.

These spectral differences are reflected in the seismic response of the five-story reinforced concrete building. Before scaling, the base shear differs by 3.05% in the X direction and 27.35% in the Y direction. Similar directional differences are observed in elastic roof displacement, with differences of 2.28% and 31.34%, respectively. The maximum inter-story drifts also differ by 2.35% in the X direction and 31.16% in the Y direction. Despite these variations, both spectra produce inter-story drifts and P-Delta stability coefficients within the adopted SNI limits. The findings show that differences in spectral characteristics can affect lateral force and deformation demands, particularly in the Y direction.

Following the required force scaling, all response spectrum cases reach the equivalent static base shear of 2961.020 kN. However, this equality results from the scaling procedure and does not eliminate differences in the vertical distribution of seismic forces. Thus, evaluating seismic response requires consideration of both spectral characteristics and the resulting structural demands rather than base shear alone. Since this study uses a single synthetic earthquake time history and one building model, the findings are limited to the analysed conditions and do not establish the developed spectrum as a substitute for a hazard-consistent design spectrum. Future research should consider additional earthquake records, independently verified ground-motion data, orthogonal horizontal components, and nonlinear time-history analysis across different building configurations.

AUTHOR'S CONTRIBUTION

Conceptualization: AR, ES
Data curation: AR, J
Formal analysis: AR
Methodology: AR, J, ES
Validation: AR, J
Visualization: AR
Writing: AR.

REFERENCES

Badan Standardisasi Nasional. (2019). SNI 1726: 2019 on Procedures for the Seismic Design of Building and Non-Building Structures *[2019 tentang Tata Cara Perencanaan Ketahanan Gempa Struktur Bangunan Gedung dan Nongedung]*. https://sitaba.pu.go.id/publikasi/6977fb4f-d02f-4fd0-a857-65219c38f24e

Badan Standardisasi Nasional. (2020). SNI 1727-2020 Minimum Design Loads and Related Criteria for Buildings and Other Structures *[2020 Beban Desain Minimum dan Kriteria Terkait untuk Bangunan Gedung dan Struktur Lain]*. https://akses-sni.bsn.go.id/dokumen/2020/SNI%201727-2020/#p=1

Budi, A. P., Jambari, J., & Pamuji, D. (2025). Strong Ground Motion Characteristics During Significant Earthquakes at BMKG Accelerograph Stations: JGPI and JBPI. *Jurnal Meteorologi Dan Geofisika*, *26*(1), 73–79. https://doi.org/10.31172/JMG.V26I1.887

Gülkan, H. P., Akansel, V. H., & Kalkan, E. (2023). Response spectrum shapes implied by earthquakes in Turkey: comparisons with design spectra. *Journal of Seismology 2023 27:4*, *27*(4), 681–692. https://doi.org/10.1007/S10950-023-10155-7

Guzel, Y., & Guzel, F. (2023). Evaluation of EC8 and TBEC design response spectra applied at a region in Turkey. *Earthquakes and Structures*, *25*(3), 199–208. https://doi.org/10.12989/EAS.2023.25.3.199

Guzel, Y., & Güzel, F. (2024). Considerations of Design Response Spectrum Involving Site Effect: Application to the Kocaeli Region, Türkiye. *Necmettin Erbakan University Journal of Science and Engineering*, *6*(1), 40–57. https://doi.org/10.47112/NEUFMBD.2024.31

Hanniel, Y., Anggraini, A., Riyanto, A., Ngadmanto, D., & Suryanto, W. (2021). Strong ground motion simulation of the 27 May 2006 Yogyakarta earthquake using Empirical Green's Function. *IOP Conference Series:*

Earth and Environmental Science, *873*(1), 012080. https://doi.org/10.1088/1755-1315/873/1/012080

Khatiwada, P., Hu, Y., Lumantarna, E., & Menegon, S. J. (2023). Dynamic Modal Analyses of Building Structures Employing Site-Specific Response Spectra Versus Code Response Spectrum Models. *CivilEng 2023, Vol. 4, Pages 134-150*, *4*(1), 134–150. https://doi.org/10.3390/CIVILENG4010009

Koz, O., Yahiaoui, A., Guntepe, S., & Celik, O. C. (2025). Exploring Why the February 6, 2023, Kahramanmaras Earthquakes Were So Destructive: Further Analysis of the SGM Data and Bidirectional Effects. *ASCE OPEN: Multidisciplinary Journal of Civil Engineering*, *3*(1), 04025015. https://doi.org/10.1061/AOMJAH.AOENG-0110

Kristiyanto, M., Pramono, S., Pariatmono, P., & Wallansha, R. (2022). *Development of the Mamuju Earthquake Elastic Response Spectrum as a Recommendation for the Response Spectrum of Buildings in Indonesia* [Pengembangan Spektra Respon Elastis Gempa Mamuju Sebagai Rekomendasi Spektra Respon Untuk Bangunan Gedung di Indonesia]. *Syntax Literate: Jurnal Ilmiah Indonesia*, *7*(2), 2929–2941. https://doi.org/10.36418/SYNTAX-LITERATE.V7I2.6363

Papazafeiropoulos, G., & Plevris, V. (2023). Kahramanmaraş—Gaziantep, Türkiye Mw 7.8 Earthquake on 6 February 2023: Strong Ground Motion and Building Response Estimations. *Buildings 2023, Vol. 13, Page 1194*, *13*(5), 1194. https://doi.org/10.3390/BUILDINGS13051194

Pawirodikromo, W. (2014). Engineering Characteristics of the 2006 Yogyakarta Earthquake Ground Motions and its Implication on the Inelastic Response of RC Structure. *Procedia Engineering*, *95*, 54–64. https://doi.org/10.1016/J.PROENG.2014.12.165

Pawirodikromo, W. (2017). Structural Dynamics Analysis *[Analisis Dinamik Struktur]*. https://scholar.google.com/citations?view_op=view_citation&hl=id&user=PmgbvXUAAAAJ&citation_for_view=PmgbvXUAAAAJ:hqOjcs7Dif8C

Prajapati, N., Shrestha, S., Ojha, K. R., Shrestha, N., & Bhatt, M. R. (2026). Development And Evaluation of Response Spectra for Gorkha Earthquake Ground Motion and Using It to Determine Seismic Response of Typical RC Building. *Journal of Science and Engineering*, *13*(1), 159–165. https://doi.org/10.3126/JSCE.V13I1.89596

Rifaldy, I., & Sukamdo, P. (2025). *Development of the Response Spectrum from the 2018 Palu Earthquake Time Series* [Pengembangan Spektrum Respons Dari Gempa Riwayat Waktu Palu 2018]. *Rekayasa Sipil*, *14*(1), 54–65. https://doi.org/10.22441/jrs.2025.v14.i1.06

Sakul, V. E., Sumajouw, M. D. J., & Manoppo, F. J. (2025). Comparison of Reinforced Concrete Structures Using Local Spectral Response Analysis, Indonesian Spectral Design and SNI 1726-2019. *COMSERVA: Jurnal Penelitian Dan Pengabdian Masyarakat*, *5*(2), 1135–1152. https://doi.org/10.59141/COMSERVA.V5I2.3281

Türkay, A. (2026). Investigation of the Effects of the 2023 Kahramanmaraş Earthquakes on Low- and Medium-Rise Reinforced Concrete Buildings. *Buildings 2026, Vol. 16, Page 1135*, *16*(6), 1135. https://doi.org/10.3390/BUILDINGS16061135

Ulza, A., Afifuddin, M., Aulia, T. B., Huzaim, H., & Abdullah, A. (2025). *Spectral Response Analysis: State-of-the-Art and Development of a Programming Framework for Computation* [Analisis Respons Spektrum: State-Of-The-Art dan Pengembangan Kerangka Pemrograman Untuk Komputasi]. *Jurnal Teknik Sipil*, *14*(1), 23–32. https://doi.org/10.24815/jts.v14i1.44764

Zengin, E., Bozorgnia, Y., Tamhidi, A., & Mazzoni, S. (2025). Spatial distribution of damage potential of the 2023 Pazarcik Turkey earthquake using inelastic-response spectra of recorded and simulated ground motions. *Earthquake Spectra*, *41*(1), 126–145. https://doi.org/10.1177/87552930241270609